

SARS-CoV-2 Envelope (E) Protein Interacts with PDZ-Domain-2 of Host Tight Junction Protein

ZO1

Ariel Shepley-McTaggart¹, Cari A. Sagum², Isabela Oliva³, Elizabeth Rybakovsky⁴, Katie DiGuilio⁴,
Jingjing Liang¹, Mark T. Bedford², Joel Cassel³, Marius Sudol⁵, James M. Mullin⁴, and Ronald N.
Harty^{1*}

¹Department of Pathobiology, School of Veterinary Medicine, University of Pennsylvania, Philadelphia, Pennsylvania, USA; ²Department of Epigenetics & Molecular Carcinogenesis, M.D. Anderson Cancer Center, University of Texas, Smithville, Texas, USA; ³The Wistar Cancer Center for Molecular Screening, The Wistar Institute, Philadelphia, PA, USA; ⁴Lankenau Institute for Medical Research, Wynnewood, Pennsylvania, USA; ⁵Department of Medicine, Icahn School of Medicine at Mount Sinai, New York, New York, USA.

***Corresponding Author:** Dr. Ronald N. Harty, Professor, Department of Pathobiology, School of Veterinary Medicine, University of Pennsylvania, 3800 Spruce Street, Philadelphia, PA 19104, USA. Phone: 215-573-4485, Fax: 215-898-7887, Email: rharty@vet.upenn.edu;

Key Words: SARS-CoV-2, COVID-19, Envelope (E) protein, ZO-1, PDZ-domain, PDZ binding motif (PBM), tight junction, virus-host interaction, antiviral therapeutic

Running Title: SARS-CoV-2 E/Host ZO-1 Interaction

Abstract: Newly emerged SARS-CoV-2 is the cause of an ongoing global pandemic leading to severe respiratory disease in humans. SARS-CoV-2 targets epithelial cells in the respiratory tract and lungs, which can lead to amplified chloride secretion and increased leak across epithelial barriers, contributing to severe pneumonia and consolidation of the lungs as seen in many COVID-19 patients. There is an urgent need for a better understanding of the molecular aspects that contribute to SARS-CoV-2-induced pathogenesis and for the development of approaches to mitigate these damaging pathologies. The multifunctional SARS-CoV-2 Envelope (E) protein contributes to virus assembly/egress, and as a membrane protein, also possesses viroporin channel properties that may contribute to epithelial barrier damage, pathogenesis, and disease severity. The extreme C-terminal (ECT) sequence of E also contains a putative PDZ-domain binding motif (PBM), similar to that identified in the E protein of SARS-CoV-1. Here, we screened an array of GST-PDZ domain fusion proteins using either a biotin-labeled WT or mutant ECT peptide from the SARS-CoV-2 E protein. Notably, we identified a singular specific interaction between the WT E peptide and the second PDZ domain of human Zona Occludens-1 (ZO1), one of the key regulators of TJ formation/integrity in all epithelial tissues. We used homogenous time resolve fluorescence (HTRF) as a second complementary approach to further validate this novel modular E-ZO1 interaction. We postulate that SARS-CoV-2 E interacts with ZO1 in infected epithelial cells, and this interaction may contribute, in part, to tight junction damage and epithelial barrier compromise in these cell layers leading to enhanced virus spread and severe respiratory dysfunction that leads to morbidity. Prophylactic/therapeutic intervention targeting this virus-host interaction may effectively reduce airway barrier damage and mitigate virus spread.

53 **Introduction:** Members of the *Coronaviridae* family are enveloped with a positive-sense single-
54 stranded RNA genome and helical nucleocapsid [1]. While symptoms in other mammalian species vary,
55 most coronaviruses cause mild respiratory disease in humans [2-4]. However, a highly pathogenic
56 human coronavirus, severe acute respiratory syndrome coronavirus (SARS-CoV-1), emerged in 2003
57 to cause acute respiratory disease in afflicted individuals [5, 6]. Moreover, in December 2019, SARS-
58 coronavirus 2 (SARS-CoV-2) emerged as the etiological agent of severe respiratory disease, now
59 called Coronavirus Disease 2019 (COVID-19), first identified in patients in Wuhan, Hubei province,
60 China. This initial outbreak has now become a global pandemic and has afflicted over 71 million people
61 and claimed over 1.6 million lives worldwide as of December 2020. The most common symptoms of
62 COVID-19 patients include fever, malaise, dry cough, and dyspnea with severe cases requiring
63 mechanical ventilation in intensive care unit (ICU) facilities for profound acute hypoxemic respiratory
64 failure [7-10]. Therefore, it is imperative to investigate how this novel SARS-CoV-2 interacts with the
65 host to cause such severe disease pathology.

66 The Spike (S), Membrane (M), Nucleocapsid (N), and Envelope (E) proteins are the four virion
67 structural proteins that are encoded within the 3' end of the viral RNA genome. The S protein is
68 responsible for entry and membrane fusion. The M protein is most abundant and gives the virion its
69 shape, while the N protein binds and protects the viral genome as part of the nucleocapsid [2, 11]. The
70 multifunctional E protein plays roles in virion maturation, assembly, and egress, and the E protein of
71 SARS-CoV-1 plays a crucial role in infection as shown by attenuated virulence *in vivo* by a SARS CoV-
72 1 virus lacking the E protein. The extreme C-terminal amino acids of the E protein of SARS-CoV-1
73 contain an important virulence factor, a PDZ domain binding motif (PBM), whose deletion reduces viral
74 virulence [11-13]. Notably, the PBM of SARS-CoV-1 E protein interacts with the PDZ domain of host
75 protein PALS1, a TJ-associated protein, leading to delayed formation of cellular TJs and disruption of
76 cell polarity in a renal epithelial model [14]. Intriguingly, the extreme C-terminal (ECT) sequence of the
77 E protein of SARS-CoV-2 is similar to that of SARS-CoV-1, suggesting that it may also interact with

78 specific host PDZ-domain bearing proteins via this putative PBM. Indeed, recent studies showed that
79 the SARS-CoV-2 E protein exhibited an increased affinity for PALS1 [9, 15].

80 We sought to determine whether the ECT of SARS-CoV-2 E protein engages specific host PDZ-
81 domain bearing TJ proteins, which may function to enhance disease progression and severity. To this
82 end, we probed a GST-fused array of approximately 100 mammalian PDZ-domains fixed on solid
83 support with biotin-labeled WT or C-terminal mutant peptides from SARS-CoV-2 E protein. Surprisingly,
84 we identified a single, robust and specific interaction between the WT E peptide and PDZ-domain #2
85 of human Zona Occludens-1 (ZO1), but not between the C-terminal mutant E peptide and ZO1. ZO1 is
86 a key scaffolding protein that organizes the formation and integrity of TJ complexes via its three PDZ
87 domains that promote multiple protein-protein interactions. Specifically, PDZ-domain #2 of ZO1 is
88 necessary to establish the characteristic continuous band of ZO1 and the TJ barrier proteins, occludin
89 and claudin-2, that is critical for the establishment of normal barrier function across an epithelium [16-
90 18, 31]. We confirmed the E-ZO1 interaction by HTRF once again demonstrating that GST-PDZ domain
91 #2 of ZO1 bound to SARS-CoV-2 E WT peptide, but not with the E mutant peptide, in a concentration
92 dependent manner.

93 Since severe pneumonia and consolidation of the lungs are often symptoms of COVID-19 [7, 8], it
94 is tempting to speculate that the SARS-CoV-2 E protein may interact with host ZO1 to disrupt or
95 damage TJ complexes and barrier function in human airway epithelial barrier cells as a mechanism to
96 enhance virus spread and disease severity. Further investigations into the interaction between SARS-
97 CoV-2 E protein and ZO1 would improve our understanding of SARS-CoV-2 virus-induced lung
98 morbidity and could be utilized to focus treatment strategies. The putative E/ZO1 interface may prove
99 to be a druggable target, and thus serve to therapeutically reduce SARS-CoV-2 transmission or disease
100 pathology.

104 **Materials and Methods:**

105 **Mammalian PDZ-domain array screen.** The PDZ domain array consisted of 90 known PDZ domains
106 and nine 14-3-3-like domains from mammalian proteins expressed in duplicate as purified GST fusion
107 proteins in lettered boxes A-J. SARS-CoV-2 E WT (Biotin-SRVKLNSSRVPDLLV-COOH) or ECT
108 mutant (Biotin-SRVKLNSSRVPAAAA-COOH) biotinylated peptides (100ug each) were fluorescently
109 labeled and used to screen the specially prepared C-terminal reading array. Fluorescent spots are
110 indicative of a positive peptide-protein interaction.

111
112 **Homogenous Time Resolve Fluorescence (HTRF).** The binding of SARS-CoV-2 WT and ECT mutant
113 E peptides (see above) to purified GST-PDZ domain #2 of ZO1 was assessed using HTRF. Both the
114 protein and the biotinylated peptides were serially diluted 1:2 in assay buffer (25 mM HEPES, pH 7.4,
115 150 mM NaCl, 5 mM MgCl₂, 0.005% Tween-20) and pre-bound for 30 min to either anti-GST-terbium
116 conjugated HTRF donor antibody or streptavidin conjugated to d2 HTRF acceptor (CisBio). Serial
117 dilutions of protein and peptides were then incubated together in a matrix format in a final volume of 10
118 uL in a white, medium binding, low volume 384-well plate. Following a 1 hr incubation, the HTRF signal
119 was measured using the ClarioStar plate reader (BMG Lab Tech). Data for the WT peptide was fit to a
120 one-site saturation binding model using XIFit (IDBS).

121
122 **Expression and Purification of GST-ZO1-PDZ-2 fusion protein.** Expression and purification of GST
123 fusion protein from pGEX-ZO1-2/3 plasmid was performed as described previously [19, 20]. Briefly, the
124 plasmids were transformed into *E. coli* BL21(DE3) cells and single colonies were cultured in 10ml of
125 LB media overnight with shaking at 37°C. The overnight culture was added into 100ml of fresh LB broth
126 and grown at 37°C for one hour with shaking. GST alone or GST-PDZ domain fusion proteins were
127 induced with isopropyl-β-d-thiogalactopyranoside (IPTG) (0.1 mM) for 4 h at 30°C. Bacterial cultures
128 were centrifuged at 5,000 rpm for 10 min at 4°C, and lysates were extracted by using B-PER bacterial
129 protein extract reagent according to the protocol supplied by the manufacturer (Pierce). Fusion proteins

130 were purified with glutathione-Sepharose 4B and eluted with elution buffer (100 mM Tris-Cl [pH 8.0],
131 120 mM NaCl, 30 mM reduced glutathione). Purified proteins were analyzed on SDS-PAGE gels and
132 stained with Coomassie blue and quantified.

133 134 **Results:**

135 Comparison of C-terminal sequences of SARS-CoV-1 and SARS-CoV-2 E proteins. The SARS-CoV E
136 protein is a small membrane protein that has multiple functions in infected cells and is incorporated into
137 mature virions [21-24]. The E protein can be divided into 3 major regions including N-terminal, trans-
138 membrane, and C-terminal domains (Fig. 1). In addition, the extreme C-terminal amino acids of SARS-
139 CoV-1 E (DLLV) comprise a validated PDZ-domain binding motif (Fig. 1, red). Since the DLLV core
140 motif is perfectly conserved in the SARS-CoV-2 E protein (Wuhan-Hu-1 strain), and the immediately
141 adjacent amino acids, although not identical, are highly conserved with those of SARS-CoV-1 E (Fig.
142 1), the likelihood that SARS-CoV-2 E protein can also interact with select PDZ-domains of host proteins
143 is high [14, 24-26].

144
145 Identification of ZO1 as a PDZ-domain interactor with the E protein of SARS-CoV-2. Here, we sought
146 to determine whether the putative PBM present within the SARS-CoV-2 E protein could interact with a
147 wide-array of host PDZ-domain containing proteins. We used fluorescently-labeled, biotinylated
148 peptides containing WT or mutated C-terminal sequences from the SARS-CoV-2 E protein to screen
149 an array composed of 90 PDZ-domains and 9 14-3-3-like domains derived from mammalian proteins
150 to detect novel host interactors (Fig. 2, top). Surprisingly, we identified a singular specific interaction
151 between the SARS-CoV-2 WT E peptide and the second PDZ-domain of human ZO1 (Fig. 2, bottom
152 left panel, red oval, position J6). As a control, the SARS-CoV-2 mutant E peptide did not interact with
153 any of the PDZ- or 14-3-3-domains present on the array (Fig. 2, bottom middle panel). All GST fusion
154 proteins were present on the array as indicated by the use of anti-GST antiserum (Fig. 2, bottom right

155 panel). To our knowledge, these results are the first to identify PDZ-domain #2 of human ZO1 as an
156 interactor with the C-terminal sequences of SARS-CoV-2 E protein.

157 158 Use of Homogenous Time Resolve Fluorescence (HTRF) to confirm the E-ZO1 interaction.

159 We sought to use a second, complementary approach to validate the E-ZO1 interaction identified in
160 our screening array. Toward this end, we used an HTRF assay to assess the binding of SARS-CoV-2
161 WT and ECT mutant E peptides to purified GST-ZO1 PDZ domain #2 (Fig. 3). Serial dilutions of GST-
162 ZO1 PDZ-domain protein and WT or mutant E peptides were incubated together for 1 hour, and the
163 HTRF signal was measured and plotted using XIFit. Indeed, we observed a clear concentration
164 dependent binding of GST-ZO1 PDZ domain #2 to WT (Fig. 3, left panel), but not the ECT mutant (Fig.
165 3, right panel), E peptide over a range of peptide concentrations. The K_d of the interaction between the
166 SARS-CoV-2 WT E peptide and a 3nM concentration of GST-ZO1 PDZ domain #2 was 29nM (Fig. 3,
167 bottom panel), which is consistent with that calculated for PDZ domains and their cognate peptides.
168 These findings confirm those described above indicating that the C-terminal sequences of SARS-CoV-
169 2 E protein interact robustly with PDZ-domain #2 of human ZO1 protein.

170 171 Discussion.

172 The coronavirus E protein has many functions during infection, including the assembly, budding, and
173 intracellular trafficking of infectious virions from the ER-Golgi complex. Modeling of the SARS-CoV-2 E
174 protein suggests that E can form a broadly cation selective ion channel with dynamic open and closed
175 states, and therefore may act as a viroporin similar to the SARS-CoV-1 E protein [21, 28]. Although the
176 genome of SARS-CoV-2 only shares about 80% identity with that of SARS-CoV-1, the ECT of the
177 SARS-CoV-2 E protein, including the DLLV core motif and adjacent amino acids, are highly conserved
178 with those of SARS-CoV-1 E protein [21-23, 25, 27] (Fig. 1). Sequence alignment of the SARS-CoV-1
179 and SARS-CoV-2 E proteins (Fig 1) highlight the sequence similarities and the putative PBM located
180 at the ECT in both proteins.

181 We utilized a screening array to identify possible host PDZ-domain containing proteins that may
182 interact with the putative PBM of the SARS-CoV-2 E protein. Excitingly, we identified a single positive
183 hit, PDZ domain #2 of TJ scaffolding protein ZO1 (Fig 2). We confirmed this novel interaction between
184 the SARS-CoV-2 E WT peptide and purified GST-PDZ domain #2 of ZO1 using HTRF (Fig 3). To our
185 knowledge, these data are the first to identify PDZ-domain #2 of ZO1 as an interactor with the ECT of
186 the SARS-CoV-2 E protein.

187 There is precedent for coronavirus E proteins interacting with host PDZ domains. Indeed, the SARS-
188 CoV-1 E protein was shown to interact with the PDZ domain of TJ protein PALS1, resulting in
189 mislocalization of PALS1 and delayed formation of TJs in a renal model. In a subsequent study, the C-
190 terminal sequences of SARS-CoV-2 E protein were also predicted to bind to the PDZ domain of PALS1
191 [14, 15]. We did not detect an E-PALS1 interaction, since the PDZ domain of PALS1 was not included
192 in the screening array (Fig 2). In addition, PDZ-domain #2 of ZO2 and ZO3 proteins were also missing
193 from our screening array. Importantly, the second PDZ domains of ZO1, ZO2, and ZO3 are fairly-well
194 conserved in their structures, and they homo- and/or hetero-dimerize to form functional multi-
195 component complexes of ZO proteins in tight junctions. Therefore, we speculate that the second PDZ
196 domains of ZO2 and ZO3 would also interact positively with the ECT of the SARS-CoV-2 E protein.

197 Several pathogens, including respiratory viruses, may cause breakdown of cellular barriers (as well
198 as cell polarity and tissue-specific unidirectional transport processes) in the lung by a mechanism
199 involving an interaction between the virus and lung epithelial cell TJs to induce leak. These pathogens
200 can interact with cellular proteins comprising TJ complexes, thereby causing their disruption and
201 subsequently enhancing systemic virus spread across epithelial and endothelial barriers [29, 30] (Fig.
202 4). There are several independent mechanisms by which an E-ZO1 interaction may disrupt TJs, barrier
203 integrity, physiologically vital transcellular transport processes, and possibly cell polarity. For example,
204 SARS-CoV-2 E protein may compete with other proteins of the TJ complex (e.g. ZO2, ZO3, or ZO1
205 itself [homodimerizing]) for binding to PDZ domain #2 of ZO1, leading to the inability of claudins to
206 organize into actual barrier-forming strands [18]. Alternatively, an E-ZO1 interaction could potentially

207 alter ZO1 binding to actin filaments of the actin-myosin ring, thereby altering barrier regulation through
208 myosin light chain kinase signaling. In addition, an E-ZO1 interaction at the TJ complex could result in
209 a decreased affinity for ZO1 binding to ZONAB (ZO1-associated nucleic acid binding protein),
210 dislocating ZONAB from the TJ complex and increasing ZONAB translocation to the nucleus, leading
211 to an increase of epithelial mesenchymal transition (EMT) and a concomitant decrease in epithelial
212 barrier function (as well as unidirectional chloride secretion) through general epithelial dedifferentiation
213 [31-33].

214 By disrupting TJ integrity, the E-ZO1 interaction would result in increased paracellular transepithelial
215 leak as well as altered unidirectional transcellular salt and water transport, contributing to accumulation
216 of water in the lungs of COVID19 patients. In fact, a recent study shows that SARS-CoV-2 infection
217 disrupts ZO1 localization, and causes barrier dysfunction as demonstrated by a decrease in
218 transepithelial electrical resistance (TEER) [34]. The authors speculate that this decrease in barrier
219 function in infected cells may be due to cytokine release in a secondary inflammatory response. It
220 remains to be determined whether an E-ZO1 interaction represents a more primary mechanism that
221 contributes to this observed decrease in barrier function and altered localization of ZO1 in infected cells
222 as described above.

223 Ongoing studies will determine whether full length SARS-CoV-2 E interacts with endogenous ZO1
224 in virus infected cells, in an effort to establish the biological significance of this virus-host interaction. In
225 addition, experiments are underway with lentivirus particles engineered to express the SARS-CoV-2
226 WT and mutant E proteins alone in human lung airway cells (Calu-3 and 16HBE) in order to investigate
227 the E/ZO1 interaction in isolation and its potential effect on TJ integrity via TEER analysis and
228 transepithelial diffusion of paracellular probe molecules. Validation of the E/ZO1 interaction in virus
229 infected cells will be important for future development of small molecule compounds to therapeutically
230 lessen lung morbidity and disease symptoms in severe COVID19 patients. Targeting the E/ZO1
231 interface for treatment may effectively reduce airway barrier cell damage and diminish the morbidity
232 and mortality associated with this major health threat.

233

234 **Acknowledgements:** The authors thank D. Argento for illustrations and graphics. Funding was
235 provided in part from a University of Pennsylvania School of Veterinary Medicine COVID-19 Pilot
236 Award, a University of Pennsylvania School of Medicine Institute for Translational Medicine and
237 Therapeutics Pilot Award, a Fast Grant from the Emergent Ventures Program at the Mercatus Center
238 at George Mason University, and NIH NIAID awards AI138052 + AI139392 to R.N.H, and a Fast Grant
239 from the Emergent Ventures Program at the Mercatus Center at George Mason University to J.M.M.
240 A.S-M. was supported in part by T32-AI070077 award from NIH/NIAID. Probing of arrayed methyl
241 reader domains was made possible via the UT MDACC Protein Array & Analysis Core (PAAC) CPRIT
242 Grant RP180804 (Directed by M.T.B). The funders had no role in study design, data collection and
243 analysis, decision to publish, or preparation of the manuscript.

244

245 **Figure Legends:**

246 **Fig. 1. Amino acid sequence of full-length SARS-CoV-1 and SARS-CoV-2 E proteins.** The N-terminal
247 (brown), trans-membrane (blue), and C-terminal (green) regions are highlighted. The conserved C-
248 terminal DLLV sequences and putative PBM motifs are shown in red.

249

250 **Fig. 2. Screening array of GST-PDZ domain fusion proteins.** The indicated GST-PDZ and GST-14-3-3
251 domain fusion proteins per lettered box were arrayed in duplicate as shown. The bottom right sample
252 (M) in each box represents GST alone as a negative control. The array was screened with biotinylated
253 E-WT or E-mutant peptides of SARS-CoV-2 E protein. Representative data for E-WT peptide (Biotin-
254 SRVKNLNSSRVPDLLV) (100µg), and E-mutant peptide (Biotin-SRVKNLNSSRVPAAAA) (100µg) are
255 shown (bottom panels). The E-mutant peptide did not interact with any GST-PDZ or GST-14-3-3
256 domain fusion proteins, whereas the E-WT peptide interacted strongly and solely with GST-PDZ
257 domain #2 from human ZO1 in position 6 in box J (red oval). A positive control for expression of all
258 GST fusion proteins is shown (anti-GST).

259

260 **Fig. 3. Homogenous Time Resolve Fluorescence (HTRF).** The concentration dependent binding
261 properties of SARS-CoV-2 E-WT (Bt-WT peptide, left panel) and E-mutant (Bt-Mut peptide, right panel)
262 peptides with purified GST-PDZ domain #2 of ZO1 are shown. Concentrations of the GST-PDZ domain
263 fusion protein ranging from 0-50 nM (indicated by the various symbols) were incubated with the
264 indicated concentrations of E-WT (left) or E-mutant (right) peptides (x-axis), and the HTRF signal was
265 measured. The E-WT peptide did not bind to GST alone (left panel, blue dots); however, clear
266 concentration dependent binding of the E-WT peptide to GST-PDZ domain 2 of ZO1 was observed.
267 The E-mutant peptide did not bind to any concentration of GST-PDZ domain 2 of ZO1 tested (right
268 panel). A K_d value of 29nM was calculated for E-WT peptide binding to 3nM concentration of GST-ZO1
269 PDZ domain #2 (bottom panel).

270

271 **Fig. 4. Model diagram of potential damage to tight junction integrity and epithelia following infection by**
272 **SARS-CoV-2. Left** – intact epithelial TJ complex and barrier function from lumen to interstitium. Cells
273 are close together with solid colored lines representing TJ proteins ZO1, ZO2, ZO3, and PALS1. **Right**
274 – compromised epithelial TJ complex (dotted colored lines) following SARS-CoV-2 infection and
275 expression of E protein resulting in barrier disruption and increased paracellular transepithelial leak.

276

277 **References.**

- 278 1. Jimenez-Guardeño JM, *et al.* Identification of the mechanisms causing reversion to virulence in an
279 attenuated SARS-CoV for the design of a genetically stable vaccine. PLoS Pathog, 2015. 11:e1005215.
- 280 2. Brian DA, Baric RS. Coronavirus genome structure and replication. Curr Top Microbiol Immunol.,
281 2005. 287, 1–30.
- 282 3. Cui J, Li F, Shi ZL. Origin and evolution of pathogenic coronaviruses. Nature Reviews. Microbiology,
283 2019. 17(3): 181–92.

- 284 4. McIntosh K. *et al.* Coronaviruses: A Comparative Review. Current Topics in Microbiology and
285 Immunology, 1974.
- 286 5. Corman, V.M., Lienau, J., and Witzentrath, M. Coronaviruses as the cause of respiratory infections.
287 Internist (Berl.), 2019. 60, 1136–1145.
- 288 6. WHO. Summary of probable SARS cases with onset of illness from 1 November 2002 to 31 July
289 2003. Retrieved from World Health Organization, who.int.com. (2004).
- 290 7. N. Zhu, *et al.* A Novel Coronavirus from Patients with Pneumonia in China. 2019. N. Engl. J. Med.,
291 2020. 382, 727–733.
- 292 8. Huang, C., *et al.* Clinical features of patients infected with 2019 novel coronavirus in Wuhan, China.
293 2020. Lancet. 10223, 497-506.
- 294 9. Chan JF, *et al.* Genomic characterization of the 2019 novel human-pathogenic coronavirus isolated
295 from a patient with atypical pneumonia after visiting Wuhan. Emerg Microbes Infect. 2020. 9(1):221-
296 236. doi: 10.1080/22221751.2020.1719902.
- 297 10. World Health Organization. Coronavirus Disease (COVID19) situation reports. Retrieved from
298 [www.who.int/publications/m/item/weekly-epidemiological-update---\(Dec 2020\)](http://www.who.int/publications/m/item/weekly-epidemiological-update---(Dec%2020)).
- 299 11. Fehr AR, Perlman S. Coronaviruses: an overview of their replication and pathogenesis. Methods
300 Mol Biol. 2015. 282:1-23. doi:10.1007/978-1-4939-2438-7_1
- 301 12. Castaño-Rodríguez C, *et al.* Role of severe acute respiratory syndrome coronavirus viroporins E,
302 3a, and 8a in replication and pathogenesis. mBio, 2018. 9:e02325-17.
- 303 13. Ruch TR, Machamer CE. The coronavirus E protein: assembly and beyond. Viruses. 2012.
304 4(3):363-382. doi:10.3390/v4030363
- 305 14. Teoh KT, *et al.* The SARS coronavirus E protein interacts with PALS1 and alters tight junction
306 formation and epithelial morphogenesis. Mol Biol Cell. 2010. 21(22):3838-52. doi: 10.1091/mbc.E10-
307 04-0338

- 308 15. Angelo Toto, *et al.* Comparing the binding properties of peptides mimicking the Envelope protein of
309 SARS-CoV and SARS-CoV-2 to the PDZ domain of the tight junction-associated PALS1 protein.
310 Protein Science, 2020. DOI10.1002/pro.3936.
- 311 16. Müller SL, *et al.* The tight junction protein occludin and the adherens junction protein alpha-catenin
312 share a common interaction mechanism with ZO-1. J Biol Chem. 2005. 280(5):3747-56. doi:
313 10.1074/jbc.M411365200.
- 314 17. Hiroaki H, *et al.* Spatial Overlap of Claudin- and Phosphatidylinositol Phosphate-Binding Sites on
315 the First PDZ Domain of Zonula Occludens 1 Studied by NMR. Molecules. 2018. 23(10):2465.
316 doi:10.3390/molecules23102465.
- 317 18.. Rodgers LS, Beam MT, Anderson JM, Fanning AS. Epithelial barrier assembly requires
318 coordinated activity of multiple domains of the tight junction protein ZO-1. J Cell Sci. 2013. 126 (Pt
319 7):1565-75. doi: 10.1242/jcs.113399.
- 320 19. Han, Z., *et al.* Modular mimicry and engagement of the Hippo pathway by Marburg virus VP40:
321 Implications for filovirus biology and budding. PLoS Pathog. 2020. 16(1): p. e1008231.
- 322 20. Liang, J., *et al.* Chaperone-Mediated Autophagy Protein BAG3 Negatively Regulates Ebola and
323 Marburg VP40-Mediated Egress. PLoS Pathog. 2017. 13(1): p. e1006132.
- 324 21. Sarkar, M., S. Saha. Structural insight into the role of novel SARS-CoV-2 E protein: A potential
325 target for vaccine development and other therapeutic strategies. Plos One. 2020. **15**(8).
- 326 22. Satarker, S., M. Nampoothiri. Structural Proteins in Severe Acute Respiratory Syndrome
327 Coronavirus-2. Archives of Medical Research. 2020. 51(6): p. 482-491.
- 328 23. Yao, H.P., *et al.* Molecular Architecture of the SARS-CoV-2 Virus. Cell. 2020. 183(3): p. 730-+.
- 329 24. Tomar, P.P.S., I.T. Arkin. SARS-CoV-2 E protein is a potential ion channel that can be inhibited by
330 Gliclazide and Memantine. Biochemical and Biophysical Research Communications. 2020. 530(1): p.
331 10-14.
- 332 25. Alam, I., *et al.* Functional Pangenome Analysis Shows Key Features of E Protein Are Preserved in
333 SARS and SARS-CoV-2. Frontiers in Cellular and Infection Microbiology, 2020. 10.

- 334 26. Toto, A., *et al.* Comparing the binding properties of peptides mimicking the Envelope protein of
335 SARS-CoV and SARS-CoV-2 to the PDZ domain of the tight junction-associated PALS1 protein.
336 Protein Science. 2020. 29(10): p. 2038-2042.
- 337 27. R. Yan *et al.* Structural basis for the recognition of SARS-CoV-2 by full-length human ACE2.
338 Science. 2020. 367, 1444–1448
- 339 28. Schoeman D, Fielding BC. Coronavirus envelope protein: current knowledge. Virol J. 2019.
340 27;16(1):69 10.1186/s12985-019-1182-0
- 341 29. Guttman JA, Finlay BB. Tight junctions as targets of infectious agents. Biochim Biophys Acta. 2009.
342 1788(4):832-41. doi: 10.1016/j.bbamem.2008.10.028.
- 343 30. Lu RY, Yang WX, Hu YJ. The role of epithelial tight junctions involved in pathogen infections. Mol
344 Biol Rep. 2014. 41(10):6591-610. doi: 10.1007/s11033-014-3543-5.
- 345 31. Heinemann U, Schuetz A. Structural Features of Tight-Junction Proteins. Int J Mol Sci. 2019.
346 20(23):6020. doi:10.3390/ijms20236020
- 347 32. Georgiadis A, Tschernutter M, Bainbridge JW, et al. The tight junction associated signalling proteins
348 ZO-1 and ZONAB regulate retinal pigment epithelium homeostasis in mice. PLoS One. 2010.
349 5(12):e15730. doi:10.1371/journal.pone.0015730
- 350 33. Balda MS, Garrett MD, Matter K. The ZO-1-associated Y-box factor ZONAB regulates epithelial cell
351 proliferation and cell density. J Cell Biol. 2003. 160(3):423-32. doi: 10.1083/jcb.200210020.
- 352 34. Hao S, Ning K, Kuz CA, Vorhies K, Yan Z, Qiu J. Long-Term Modeling of SARS-CoV-2 Infection
353 of In Vitro Cultured Polarized Human Airway Epithelium. mBio. 2020. 11(6):e02852-20.
354 doi:10.1128/mBio.02852-20

Figure 1

SARS-CoV-1 E protein

¹MYSFVSEETGTLIVNSVLLFLAFVVFLVTLAILTALRLCAYCCNIV
NVSLVKPTVYVYSRVKNLNSSEGVPDLLV⁷⁶

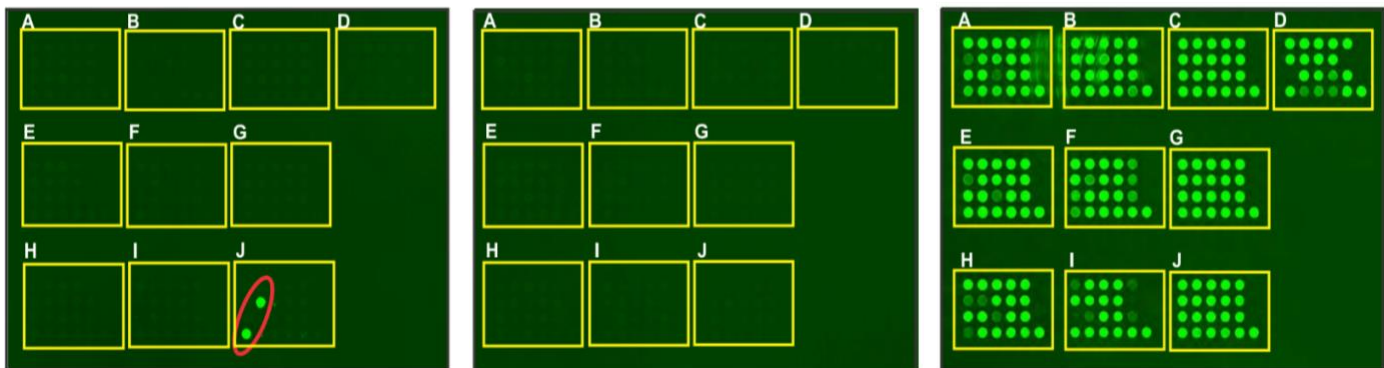
SARS-CoV-2 E protein

¹MYSFVSEETGTLIVNSVLLFLAFVVFLVTLAILTALRLCAYCCNI
VNVSLVKPSFYVYSRVKNLNSSRVPDLLV⁷⁵

Figure 2

<p>PDZ</p> <p>A 1) α-1-syntrophin (1/1)/Q61234 A 2) β1-syntrophin (1/1)/Q99L88 A 3) γ1-syntrophin (1/1)/Q925E1 A 4) γ2-syntrophin (1/1)/Q925E0 A 5) Chapsyn-110 (2/3)/Q91XM9 A 6) Chapsyn-110 (3/3)/Q91XM9 A 7) Dlg3 (1/1)/Q6XE40 A 8) Dvl1 (1/1)/Q60838 A 9) Dvl2 (1/1) A 10) Dvl3 (1/1)</p>	<p>PDZ</p> <p>B 1) Cipp (3/10)/Q63ZW7 B 2) Cipp (5/10)/Q63ZW7 B 3) Cipp (8/10)/Q63ZW7 B 4) Cipp (9/10)/Q63ZW7 B 5) Cipp (10/10)/Q63ZW7 B 6) Radil (1/1)/Q69Z89 B 7) Erbin (1/1)/Q80TH2 B 8) GRASP55 (1/1)/Q99JX3 B 9) Grip1 (6/7)/Q925T6 B 10) Grip2 (5/7)/E0CX54</p>	<p>PDZ</p> <p>C 1) Harmonin (2/3)/Q9ES64 C 2) HtrA1 (1/1)/Q9QZK6 C 3) HtrA3 (1/1)/Q9D236 C 4) Interleukin 16 (1/4)/Q9QZP6 C 5) LARG (1/1)/Q8R4H2 C 6) LIN-7A (1/1)/Q8JZS0 C 7) Lin7c (1/1)/O88952 C 8) Lnx1 (2/4)/O70263 C 9) Lnx1 (3/4)/O70263 C 10) Lrrc7 (1/1)/Q80TE7</p>	<p>14-3-3 / 14-3-3 like</p> <p>D 1) sigma/NP_006133 D 2) beta/alpha/NP_647539.1 D 3) epsilon/NP_006752 D 4) gamma/CAG46702 D 5) eta/CAG30498 D 6) theta/NP_006817 D 7) zeta/delta/NP_663723 D 8) SMG5/NP_056142 D 9) SMG7/NP_963862</p>
<p>PDZ</p> <p>E 1) Magi-1 (2/6)/Q6RHR9 E 2) Magi-1 (4/6)/Q6RHR9 E 3) Magi-1 (6/6)/Q6RHR9 E 4) Magi-2 (2/6)/Q9WVQ1 E 5) Magi-2 (5/6)/Q9WVQ1 E 6) Magi-2 (6/6)/Q9WVQ1 E 7) Magi-3 (5/6)/Q9EQJ9 E 8) Mals2 (1/1)/lin-7/Q9HAP6 E 9) Magi-3 (1/6)/Q9EQJ9 E 10) Semcap3 (1/2)/Q69ZS0</p>	<p>PDZ</p> <p>F 1) Mpp7 (1/1)/Q8BVD5 F 2) MUPP1 (5/13)/Q8VBX6 F 3) MUPP1 (10/13)/Q8VBX6 F 4) MUPP1 (11/13)/Q8VBX6 F 5) MUPP1 (12/13)/Q8VBX6 F 6) MUPP1 (13/13)/Q8VBX6 F 7) nNOS (1/1)/Q9Z0J4 F 8) OMP25 (1/1)/Q8K4F3 F 9) PAR-3 (3/3)/Q99NH2 F 10) Shank3 (1/1)/Q4ACU6</p>	<p>PDZ</p> <p>G 1) NHERF-1 (1/2)/P70441 G 2) NHERF-1 (2/2)/P70441 G 3) NHERF-1 FL/P70441 * G 4) NHERF-2 (1/2)/Q9JHL1 G 5) NHERF-2 (2/2)/Q9JHL1 G 6) NHERF-2 FL/Q9JHL1 * G 7) Pdzk1 (1/4)/NHERF-3/Q9JIL4 G 8) Pdzk1 (3/4)/NHERF-3/Q9JIL4 G 9) Pdzk3 (1/4)/NHERF-4/Q99MJ6 G 10) Pdzk3 (3/4)/NHERF-4/Q99MJ6</p>	
<p>PDZ</p> <p>H 1) PAR6B (1/1)/Q9JK83 H 2) Pdlim5 (1/1)/Q3UGD0 H 3) Pdzk11 (1/1)/Q9CZG9 H 4) PDZ-RGS3 (1/1)/Q9DC04 H 5) PSD95 (1/3)/Q62108 H 6) PSD95 (2/3)/Q62108 H 7) PSD95 (3/3)/Q62108 H 8) PTP-BL (2/5)/Q64512 H 9) PAR3B (1/3)/Q5SV53 H 10) TIP-1 (1/1)/Q9DBG9</p>	<p>PDZ</p> <p>I 1) SAP102 (2/3)/P70175 I 2) SAP102 (3/3)/P70175 I 3) SAP97 (1/3)/Q811D0 I 4) SAP97 (2/3)/Q811D0 I 5) SAP97 (3/3)/Q811D0 I 6) Scrb1 (3/4)/Q80U72 I 7) Shank1 (1/1)/D3YZU1 I 8) Pdzk3 (1/6)/E9Q1M1 I 9) Pdzk3 (2/6)/E9Q1M1</p>	<p>PDZ</p> <p>J 1) Shroom (1/1)/Q9QXN0 J 2) SLIM (1/1)/Q8R1G6 J 3) Tiam2 (1/1)/Q6ZPF3 J 4) Whirlin (3/3)/Q5MLF8 J 5) ZO-1 (1/3)/P39447 J 6) ZO-1 (2/3)/P39447 J 7) ZO-2 (1/3)/Q9Z0U1 J 8) ZO-3 (1/3)/Q9QXY1 J 9) Scrb1 (1/4)/Q80U72 J 10) Scrb1 (2/4)/Q80U72</p>	

*= Non-Codon Optimized Construct



E-WT peptide

E-mutant peptide

anti-GST

Figure 3

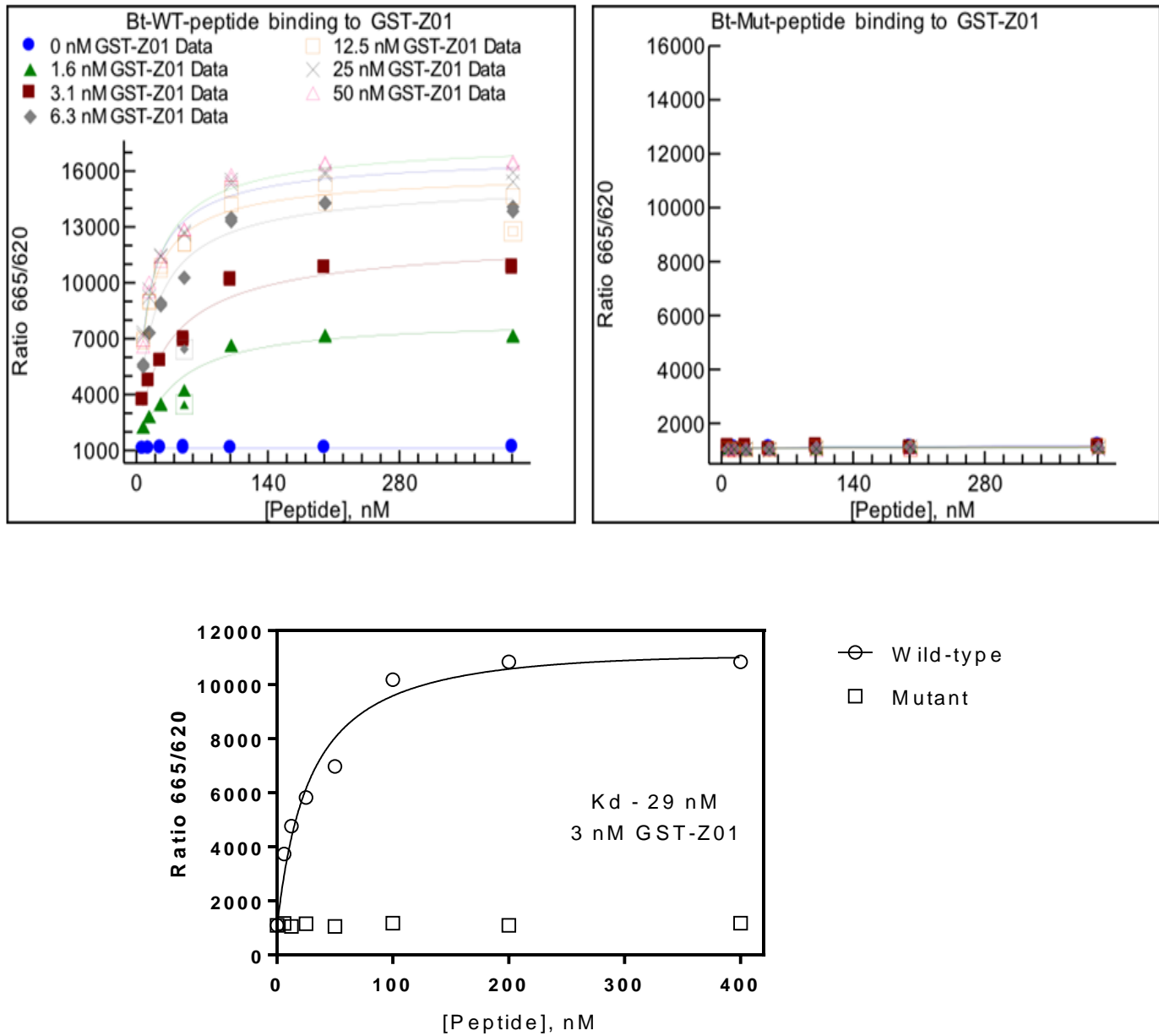


Figure 4

